IOP Publishing Plasma Sources Science and Technology

Plasma Sources Sci. Technol. **24** (2015) 025037 (8pp) doi:10.1088/0963-0252/24/2/025037

Collisionless sheath heating in current-driven capacitively coupled plasma discharges via higher order sinusoidal signals

S Sharma[1], S K Mishra[1], P K Kaw[1], A Das[1], N Sirse[2] and M M Turner[2]

[1] Institute for Plasma Research (IPR), Gandhinagar-382428, India
[2] National Centre for Plasma Science & Technology, Dublin City University (DCU), Dublin, Ireland

E-mail: nishfeb@gmail.com

Received 21 October 2014, revised 27 January 2015
Accepted for publication 20 February 2015
Published 7 April 2015

Abstract

Collisionless heating of the electrons in the vicinity of the sheath region corresponding to higher order sinusoidal signals in a current-driven radio-frequency capacitively coupled plasma discharge has been investigated analytically and further verified by *particle-in-cell simulation*. The simulation results for collisionless sheath heating are found to be in good agreement with analytical predictions. In contrast to the voltage driven case, it is demonstrated that a pure sinusoidal waveform gives maximum electron sheath heating with a current-driven configuration and the ion energy can be controlled by varying the pulse width.

Keywords: stochastic heating, CCP discharge, RF sheath, higher order sinusoidal waveform

(Some figures may appear in colour only in the online journal)

1. Introduction and motivation

In recent studies [1–10] it is proposed that better separate control over ion flux and energy in capacitively coupled plasma (CCP) discharges can be achieved by applying non-harmonic, tailored or multi-frequency signals over electrodes; such discrete control over ion flux and energy is not possible in conventional single-frequency CCP discharges where coupling between them limits its utility [1]. The control over the etching rate and uniform deposition of ions is of immense importance on account of its wide applicability in numerous material processing applications [1]. In principle, in conventional CCP discharges, the use of multiple harmonic/non-sinusoidal signals causes electrical asymmetry and sets a finite dc field between the electrodes [3–7] which allows additional control of bias voltage (ion energy), keeping the plasma density constant. In general these investigations [7–16] take account of dual/triple/multiple-frequency voltage-driven cases where the applied fundamental signal is assisted by even/odd harmonics and the phase difference between them is tuned to control the desired ion flux or energy.

Conventional radio-frequency (RF) CCP discharges can operate in two configurations, namely voltage and current driven sources; an important feature of RF-CCP discharge is that it may operate even at low pressure (~mTorr) where discharge is primarily sustained by stochastic (or collisionless) heating [17–27]. Of course the collisions cannot be avoided in realistic scenarios; however there are physical situations like sheath formation in very low pressure CCP-discharges where the mean free path of electrons is large (~few cm) enough and the collisional heating is insignificant in comparison to stochastic heating; in fact this is the case considered in the present study. The physical description of the sheath region dynamics become more simplified [17–27] with this consideration of a collisionless system. In a recent analysis [28], the effect of a non-sinusoidal (Gaussian in particular) voltage waveform pulse on the power deposition has been explored on the basis of a particle-in-cell (PIC) simulation. For illustration of the effect, the authors [28] have used a finite width voltage pulse waveform of a Gaussian profile, namely $V = V_0 \exp[-\alpha(t - t_0)^2]$ with a characteristic frequency of $f = 13.56$MHz where the pulse width is characterized by parameter α, and V_0 refers to the maximum voltage amplitude at a mean time t_0. It is demonstrated that electron heating can directly be controlled by changing the Gaussian pulse width; this enhancement in electron sheath heating modifies

the plasma density and ion flux for same operating conditions. This effect can be understood in terms of the discrete Fourier transform (DFT) of the potential waveform which is eventually characterized by the manifestation of higher harmonics, in addition to the fundamental applied frequency; the composition of higher harmonics increases with decreasing pulse width. The applied potential drives a current (J) consistent with the Maxwell–Ampère law which increases with increasing frequency [29]. Thus the large heating of electrons with decreasing pulse width can be attributed to the enhancement in the current associated with the inclusion of higher harmonics in the applied potential waveform. This leads the system to operate in a mode where the ion flux is controlled by tuning the width of the Gaussian pulse, keeping the ion energy (i.e. the potential across the sheath) constant [30]. However, concerning any practical application of the tailored (voltage) waveforms, the power matching [16] characterizing the coupling of applied power with the plasma through the electrodes is a crucial technical issue of significant interest. Most of the experimental work [14, 15] ignores this fact where it causes the high reflectance of the input power; this is certainly intolerable on industrial scales.

Although the practical CCP discharges are voltage driven, most of the analytical studies on sheath dynamics and stochastic (collisionless) heating of electrons in the vicinity of the sheath region are based on current-driven sources [1, 17–27]. Collisionless sheath heating is a kinetic phenomenon which occurs as a consequence of the mutual interaction between the expanding/collapsing phase of the sheath in response to the applied oscillatory RF field and plasma electrons. The experimental [31, 32] and analytical [17–25] prediction of the energy deposition in low pressure discharges due to stochastic heating mechanisms in the vicinity of the sheath is also verified by self-consistent PIC simulations [23]. In this analysis our concern is to explore the physics of the effect produced by non-sinusoidal perturbations on stochastic or collisionless sheath heating for current-driven CCP discharges, and to investigate whether the effects similar to those of voltage-driven cases [28] can also be generated with current-driven sources; in such a case one can expect to tune the ion energy (etching rate) via varying the pulse width. The outcome may be conceived as a conceptual basis to utilize it further for realistic situations and industrial applications.

In order to illustrate the conceptual basis, here we analyze the situation where the CCP discharge operates in a collisionless regime with higher order sinusoidal current-driven sources, and explore its consequences on sheath structure, collisionless electron-sheath heating, and power absorption by electrons; these effects are further verified with particle-in-cell simulation results. For analytical convenience we have chosen a periodic higher order sinusoidal waveform as an applied current and the algebraic expression for the transient profile can be written as

$$J(x) = J_0 \sin^{2\alpha+1}(\omega t), \tag{1}$$

where J_0 and $\omega(= 2\pi f)$ are the amplitude and frequency of the applied current density, $(2\alpha + 1)$ refers to the order of the applied sinusoidal profile, and α is the parameter which controls the mean width of the pulse and takes integral values. The time dependence of different order profiles are displayed in figure 1; a train of such pulses is applied to the electrodes and the system is left to evolve with time to achieve a steady-state situation.

As is evident from the current density profile (i.e. equation (1)), the pulse mean width decreases with increasing α and the corresponding DFT suggests the occurrence of higher harmonics of applied fundamental frequency with decreasing pulse width. The heating of electrons in the sheath region in this case can be attributed to the effect of such higher harmonics on sheath dynamics; sheath dynamics in RF-CCP discharges driven by current driven sources has extensively been explored in literature [17–25]. The net power deposited in the vicinity of the RF sheath driven by a pure sinusoidal current profile (i.e. $\alpha = 0$) in a collisionless regime has been estimated by Lieberman [1] and can be expressed as

$$S_{\text{stoc}} = (3\pi H/32)(m_{\text{e}}\, n_0 u_{\text{e}} u_0^2), \tag{2}$$

where $u_e[= (8eT_{\text{e}}/\pi m_{\text{e}})^{1/2}]$ is the mean thermal velocity of electrons, n_0 and u_0 refer to the density and drift velocity of electrons at the ion sheath edge respectively, T_{e} and m_{e} correspond to the mean temperature (in eV) and mass of electrons respectively, e is the electronic charge, $H(= J_0^2/\pi\varepsilon_0\, eT_{\text{e}}\, \omega^2\, n_0)$ refers to a dimensionless sheath controlling parameter, and $u_0(= J_0/n_0\, e)$.

Intuitively, one can conclude (from equation (2)) that in the case of a current-driven CCP discharge the electron sheath heating decreases with an increase in the contribution of higher harmonics in the current waveform. Another notion comes from the Kaganovich [22] interpretation of electron sheath collisionless heating in current-driven CCP discharges where the energy deposition is determined by a velocity kick ($\delta u_s \propto 1/\omega^2$) gained by electrons interacting with an oscillating sheath. This reveals the fact that large velocity kicks i.e. low frequency drivers, gives rise to a large heat deposition in the sheath region. In the next section an analytical formulation for the evaluation of collisionless heating for a higher order sinusoidal profile in current-driven CCP discharges has been established which is primarily an extended version of the analysis by Lieberman [17] and Kaganovich *et al* [23]. The simulation scheme utilized for the validation of the present concept and relevant parameters has briefly been described in section 3. The physical interpretation and discussion of the results based on analysis and numerical simulation is made in section 4. A summary of the outcome concludes the paper.

2. Sheath structure and collisionless sheath heating of electrons

In order to analyze the sheath structure and consequent stochastic (collisionless) heating of electrons in the proximity of the sheath region in a CCP discharge, driven by higher order sinusoidal current waveforms, we utilize the formalism adopted by Lieberman [17] and Kaganovich *et al* [23] in the case of a pure sinusoidal current profile. We have used

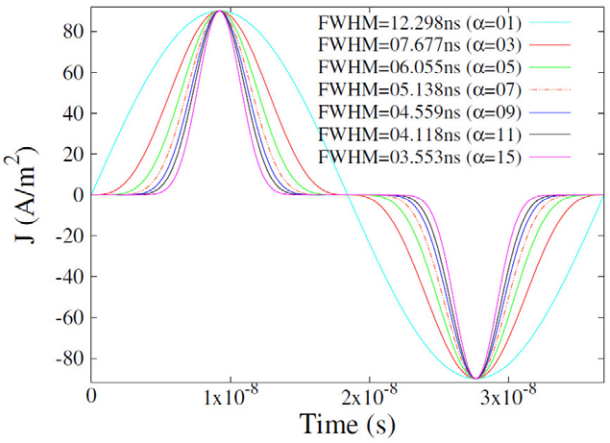

Figure 1. Time profile of the higher order sinusoidal current profile for different pulse widths.

the same schematic diagram illustrated as figure 1 in [17] to describe the RF sheath structure in the present analysis. The Maxwell equation for the instantaneous electric field (E) in the sheath region can be expressed as

$$(\partial \overline{E}/\partial x) = (e/\varepsilon_0) n_i(x), \quad s(t) < x \\ = 0 \quad s(t) > x. \tag{3}$$

Here $s(t)$ refers to the distance from the ion sheath edge (at $x = 0$) to the electron sheath edge, x is an arbitrary position in the sheath region, and ε_0 is the permittivity of free space. Following the algebraic treatment of Lieberman [17], the equations governing the sheath structure and electron sheath motion can be written as

$$(\mathrm{d}\overline{E}/\mathrm{d}x) = (e/\varepsilon_0)\,[n_i(x) - \overline{n}_e(x)], \tag{4}$$

$$(\mathrm{d}\overline{\varphi}/\mathrm{d}x) = -\overline{E}, \tag{5}$$

$$\overline{n}_e\,(x) = [1 - (\gamma/\pi)] n_i\,(x), \tag{6}$$

$$n_i\,(x) = n_0(1 - 2\overline{\varphi}/T_e)^{-1/2} \tag{7}$$

and

$$n_i\,(x) u_s = n_i\,(x)(\mathrm{d}s/\mathrm{d}t) = n_0 u_0 \sin^{2\alpha+1}\omega t, \tag{8}$$

where E, φ and n_e/n_i are the electric field, potential and electron/ion density respectively; the bar on these quantities corresponds to the time-averaged values over one RF cycle, n_0 is the mean density of the electrons/ions in bulk (ion sheath edge), u_s is the velocity of the electron sheath edge while $u_0 = (J_0/en_0)$, and γ refers to the arbitrary phase associated with position x in the sheath region.

The above written equations are primarily the manifestation of Poisson's equation and the conservation of the number and energy of ions along with the electron sheath dynamics. Following the algebraic steps given in [17], one can combine the space and time integrations of equations (3) and (8) respectively to obtain the instantaneous electric field as

$$E(x,\omega t) = \frac{e}{\varepsilon_0}\int_0^x n_i\,(\varsigma)\mathrm{d}\varsigma \\ - J_0\varepsilon_0\omega\left[\frac{\pi^{1/2}\Gamma(1+\alpha)}{2\Gamma(3/2+\alpha)} - \left({}_2F_1\left[\frac{1}{2}, -\alpha, \frac{3}{2}, \cos^2\omega t\right]\right)\cos\omega t\right] s(t) < x \\ = 0 \qquad\qquad s(t) > x \tag{9}$$

where ${}_2F_1[...]$ is the hyper-geometric function. Integrating equation (9) over an RF period, the time-averaged electric field ($\overline{E}$) at any position x in the sheath can be written as

$$\overline{E}(x) = -(\mathrm{d}\overline{\varphi}/\mathrm{d}x) = (1/2\pi)\int_{-\gamma}^{\gamma} E(x,\omega t)\mathrm{d}(\omega t) \\ = \left(\frac{J_0\gamma}{\pi\varepsilon_0\omega}\right)\left[-\gamma\left({}_2F_1\left[\frac{1}{2}, -\alpha, \frac{3}{2}, \cos^2\gamma\right]\right)\cos\gamma \right. \\ \left. + (1/2)\int_{-\gamma}^{\gamma}\left({}_2F_1\left[\frac{1}{2}, -\alpha, \frac{3}{2}, \cos^2\gamma\right]\right)\cos\gamma\,\mathrm{d}\gamma\right]. \tag{10}$$

Using equations (7) and (8) in limiting conditions, namely $x = s$ and $\omega t = \gamma$ at any particular x in the sheath region, one obtains

$$(\mathrm{d}\gamma/\mathrm{d}x) = (1 - 2\overline{\varphi}/T_e)^{-1/2}/s_0 \sin^{2\alpha+1}\gamma, \quad \text{with } s_0(= J_0/n_0\, e\omega). \tag{11}$$

The above equations (i.e. equations (10)–(11)) yield a self-consistent description of the RF sheath and can easily be solved to obtain the potential structure; other physical parameters can easily be derived from equations (5)–(7). Dividing equation (10) by equation (11) and integrating with appropriate boundary conditions, namely $\overline{\varphi} = 0$ at $\gamma = 0$, one gets the time-averaged potential

$$(1 - 2\overline{\varphi}/T_e)^{1/2} = 1 - H\int\gamma\sin^{2\alpha+1}\gamma\left({}_2F_1\left[\frac{1}{2}, -\alpha, \frac{3}{2}, \cos^2\gamma\right]\right)\cos\gamma\,\mathrm{d}\gamma \\ + (H/2)\int\sin^{2\alpha+1}\gamma\left[\int_{-\gamma}^{\gamma}\left({}_2F_1\left[\frac{1}{2}, -\alpha, \frac{3}{2}, \cos^2\omega t\right]\right)\cos\omega t\,\mathrm{d}(\omega t)\right]\mathrm{d}\gamma \tag{12}$$

where $H(= s_0^2/\pi\lambda_d^2)$ and $\lambda_d[= (\varepsilon_0 T_e/en_0)^{1/2}]$ is the Debye length.

Substituting for $\overline{\varphi}$ from equation (12) in equation (11) and integrating it again with the initial boundary conditions $\gamma = 0$ at $x = 0$, one can write

$$\frac{x}{s_0} = \int\sin^{2\alpha+1}\gamma\left(1 - H\int\gamma\sin^{2\alpha+1}\gamma\left({}_2F_1\left[\frac{1}{2}, -\alpha, \right.\right.\right. \\ \left.\left.\left.\frac{3}{2}, \cos^2\gamma\right]\right)\cos\gamma\,\mathrm{d}\gamma\right)\mathrm{d}\gamma \\ + \int\sin^{2\alpha+1}\gamma\left((H/2)\int\sin^{2\alpha+1}\gamma\left[\int_{-\gamma}^{\gamma}\left({}_2F_1\left[\frac{1}{2}, -\alpha, \right.\right.\right.\right. \\ \left.\left.\left.\left.\frac{3}{2}, \cos^2\omega t\right]\right)\cos\omega t\,\mathrm{d}(\omega t)\right]\mathrm{d}\gamma\right)\mathrm{d}\gamma. \tag{13}$$

The above equation (i.e. equation (13)) represents the self-consistent nonlinear evolution of the oscillatory motion of the electron sheath. Similarly the mean (time-averaged) electron density and ion density can be obtained by using equation (12) with equations (6) and (7) respectively. The expressions derived (equations (9)–(13) are in a generalized form and can be solved analytically/numerically for any arbitrary higher order (α) sinusoidal current waveform; it is further verified that the expressions corresponding to pure sinusoidal waveforms can be retained by putting $\alpha = 0$ in the above equations (namely equations (11)–(13). The self-consistent nonlinear evolution of the oscillatory motion of the sheath, based on analytical treatment as a function of phase (γ) for different orders (α) of applied sinusoidal current waveform has been displayed in figure 2(a); the space evolution of the corresponding mean electric field ($\overline{E}$) and mean electric potential ($\overline{\varphi}$) in the sheath has been illustrated in figures 2(b) and (c) respectively. The results shown in the figures correspond to the expanding phase (i.e. $0 \leqslant \gamma \leqslant \pi$) of the sheath and one can anticipate symmetrical behaviour in the collapsing phase (i.e. $\pi \leqslant \gamma \leqslant 2\pi$). The figures indicate that the sheath width (x) decreases with increasing α; consequently the magnitudes of $\overline{E}$ and $\overline{\varphi}$ corresponding to a maximum sheath expansion also display similar dependence on α.

The plasma electrons interacting with the moving sheath experience a change in their kinetic energy; as the electron and sheath approach each other, the electron gains energy, while it loses energy as they are in same phase. For an oscillatory motion of the electron sheath edge, a fraction of electrons lose their energy to the sheath in the collapsing phase, while some electrons gain energy from the expanding sheath. In this process the electrons effectively gain finite energy in an RF period; considering the sheath structure and its oscillatory motion on the basis of kinetic theory, Lieberman [17] has estimated the average energy gain (stochastic heating) by electrons in the case of a pure sinusoidal current waveform. Following a kinetic approach similar to that of Lieberman [17], the generalized expression for stochastic heating in the case of a higher order sinusoidal waveform can be written as

$$S_{\mathrm{GL}} = m_{\mathrm{e}}\, u_{\mathrm{e}} \langle (u_{\mathrm{s}} - v_{\mathrm{o}}) n_{\mathrm{s}}\, u_{\mathrm{s}} \rangle_{\gamma} = m_{\mathrm{e}} n_0 u_{\mathrm{e}} u_0^2 \, \langle (u_{\mathrm{s}} - v_{\mathrm{o}}) \sin^{2\alpha+1}\gamma \rangle_{\gamma}, \tag{14}$$

where v_{o} refers to the time varying oscillatory velocity of the plasma electrons (at the ion sheath edge) under influence of the applied RF current and can be expressed as

$$(v_{\mathrm{o}}/u_0) = (\omega_{\mathrm{p}}^2/\omega^2) \int_0^{\gamma} ({}_2F_1[1/2, -\alpha, 3/2, \cos^2\gamma]) \cos\gamma \, \mathrm{d}\gamma \tag{15}$$

where $\omega_{\mathrm{p}} (= n_0 e^2/\varepsilon_0 m_{\mathrm{e}})^{1/2}$ is the plasma frequency at the ion sheath edge.

However, in deriving stochastic sheath heating, the effect of an applied field on the motion of bulk electrons is ignored, which leads to inconsistency in current conservation at the electron sheath edge [20, 24]. This fact has been incorporated by Kaganovich *et al* [23] in their analysis and the electron-sheath dynamics are formulated in the reference frame where bulk electrons exhibit a non-drifting nature; it is concluded

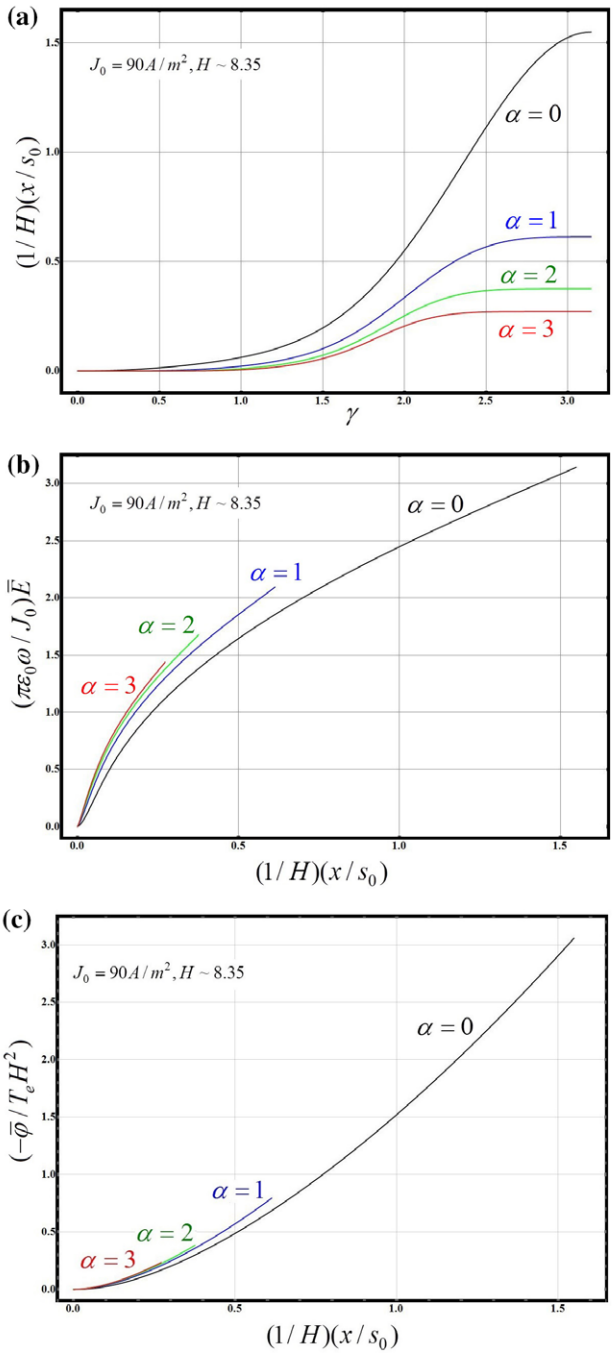

Figure 2. (a) Normalized position (x) of RF electron sheath as a function of phase (γ) for different order sinusoidal current profiles. (b) Normalized mean electric field ($\overline{E}$) as a function of normalized position (x) for different order sinusoidal current profiles. (c) Normalized mean electric potential ($\overline{\varphi}$) as a function of normalized position (x) for different order sinusoidal current profiles.

that the Lieberman expression overestimates the stochastic heating for low H values in the case of a pure sinusoidal current profile. Including this effect of oscillatory motion of bulk electrons, and following the Kaganovich treatment, the expression for stochastic sheath heating in the present case gets modified as

$$S_{\mathrm{GK}} = m_{\mathrm{e}}\, n_0\, u_{\mathrm{e}} u_0^2 \, \langle (u_{\mathrm{s}} - v_{\mathrm{o}})^2 \, (n_{\mathrm{i}}/n_0) \rangle_{\gamma}. \tag{16}$$

For a specific higher order sinusoidal current profile (α) the collisionless heating of electrons can be obtained by substituting the appropriate expressions for v_o (from equation (15)) and ion density (n_i, from equation (7)); it is also verified that sheath heating expressions (i.e. equations (14), (16) with $\alpha = 0$ readily reduce to the known expressions for a pure sinusoidal current driven case, derived in previous analyses [17, 23, 24].

3. Simulation scheme and parameters

For numerical appreciation of the conceptual basis, a simulation code based on a semi-infinite PIC scheme [33, 34] has been used to investigate the average collisionless heating of electrons near the localized sheath region in the steady state. A semi-infinite PIC technique is a simplified version of the standard full PIC scheme and applicable in analyzing plasma behaviour in the sheath region and bulk plasma in its vicinity. From the physics perspective, in such modifications the system length is considered to be long enough so that the particles carrying the influence of one (say right) electrode from the sheath region (i.e. electrode boundary) get diminished within a few (say ~5) sheath widths and therefore long before reaching the left electrode of the simulation regime; thus the effect of one electrode is not sensed by the other electrode. Hence the combination of a powered electrode, sheath and finite region of the bulk can be considered as a semi-infinite simulation box, and this is the case considered in our present analysis; this consideration facilitates computations with large resolution for data analysis in the vicinity of the sheath region with the same computational resources. Our PIC simulation box (~6 cm) is considered to consist of charged plasma (argon) particles (electrons/ions) to begin with; further, the mean free path of the electrons/ions is chosen to be larger than the system length and the inter-particle collisions between electrons–ions–neutrals are ignored.

The equilibrium of the system is maintained by adding the charged particles characterized by a drifting Maxwellian distribution from the bulk boundary in a manner consistent with the boundary condition. The right boundary is considered as a perfectly absorbing electrode driven by an RF current and the particles that hit any of the boundaries get absorbed in the simulation. The electrons and ions are loaded from the bulk (left) boundary continuously in order to replace the charged particles lost over the simulation boundaries and conserve the total current at each time step; the electrons/ions added from the bulk edge takes account of the role played by ionization in real systems in order to maintain the plasma density at a constant level in the steady state. Thus the constancy of plasma (ion) density is an inherent feature of the algorithm developed for the semi-infinite PIC simulation technique and certainly characterizes the steady state of the system. The only feature missing from such a study is the distribution of the ionization source, which would be over the whole volume of the discharge for a typical ionization model, and is localized at the bulk boundary in the present simulation; since the collisional mean free path is very long, this does not make much difference from the physics point of view. As the next step, the simulation is left to evolve until a steady state profile of the system is achieved; the detailed description of the simulation approach can be seen in [33, 34]. The utility of the semi-infinite particle-in-cell code in this particular collisionless regime is also established in literature [20, 24–27, 33–38] published in recent years. In this particular analysis, the sheath dynamics in the simulation box of finite length (6 cm long) and filled with argon (Ar) plasma is considered to be driven by an RF current source (as indicated in equation (1)), characterized by frequency ($f = 27.12$ MHz). The simulation is performed for the following set of discharge plasma parameters [26]

$$J_0 = 90\,\mathrm{A\,m^{-2}}, n_e \approx n_i = 3\times10^{15}\,\mathrm{m^{-3}}, \quad T_e = 2.5\,\mathrm{eV}$$
$$\text{and } T_i = 0.03\,\mathrm{eV}.$$

The simulation results for various order non-sinusoidal waveforms have been compared with the analytical predictions. It is necessary to mention here that in a typical low pressure CCP discharge (collisionless regime), the electrons in the vicinity of the sheath exhibit non-Maxwellian EEDF (electron energy distribution function) and the temperature cannot be exactly defined; for the sake of simplicity in our simulation model the mean random energy plays a role similar to the effective temperature.

4. Numerical results and discussion

As an RF electric field (driven by a current source in this analysis) is applied to an electrode, the plasma electrons are exposed to a time dependent electric field and instantaneously respond with field oscillations. This external field naturally gets shielded by plasma over a characteristic length of the order of a few Debye lengths over the electrode, and the plasma density self-consistently decays in order to maintain the electrode at a floating potential. The sheath heating in the PIC simulation analysis is determined by time/space averaging of the product of the local current density with the local effective electric field ($J.E$) over an RF cycle (i.e. over an RF period). Figure 3 illustrates the spatio-temporal evolution (colour scale) of the stochastic (collisionless) heating of electrons in an RF cycle in a current-driven CCP discharge for different pulse widths of higher order sinusoidal profiles. In general, in an RF cycle the electrons interacting with the expanding sheath get positive kicks and gain positive energy while the particles lose their energy in the collapsing phase of the sheath; this nature of positive and negative heating can be seen by the red and blue patches in the vicinity of the sheath edge respectively. The larger mean width, namely full width half maximum (FWHM), associated with the applied waveforms (referred to in equation (1)) causes the slow expansion/collapse of the oscillating sheath and provides a large interaction time to the electrons hitting the sheath edge. This results in the large stochastic heating of electrons in the pure sinusoidal waveform in comparison to higher order sinusoidal cases (smaller mean width), as displayed in figure 3. The figure also shows some high frequency oscillations in the heating for the pure sinusoidal case (in the proximity of the sheath) and this effect is less prominent in the higher order sinusoidal profiles; such an effect has also been predicted by Schulze [39] and Sharma and Turner [40] in their

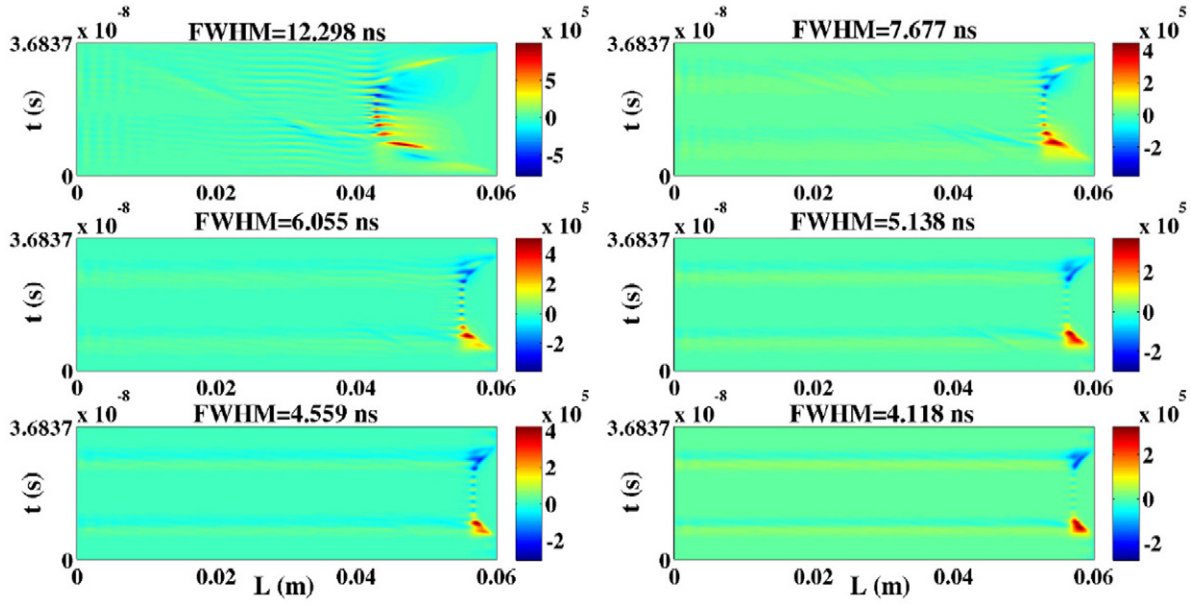

Figure 3. Spatio-temporal evolution of sheath heating for different pulse width corresponding to different order sinusoidal current profiles.

PIC simulations. These filamentary structures are understood to be the source of excitation of transient field structures which carry the energy from the oscillating sheath to the bulk [29, 41] and redistribute this energy to plasma particles via the phase mixing mechanism [22], as in case of Landau damping. We would like to state here that this phenomenon is primarily a kinetic effect and the details of the mechanism are still to be worked out. The particle simulation also reveals the fact that the collisionless sheath heating decreases with decreasing the mean pulse width; the pulse width is described here via FWHM. It also concludes that the pure sinusoidal pulse (i.e. $\alpha = 0$, FWHM ~12.3 ns) exhibits the maximum electron sheath heating.

The space evolution of time-averaged electron sheath heating corresponding to a higher order sinusoidal profile (equation (1)) has been displayed in figure 4. The electron sheath heating peaks at finite distance from the electrode in the sheath region; this can be understood in terms of a mutual competitive phenomena of decreasing the local electric field and increasing plasma density ($J.E \propto n_e E^2$). Similar behaviour of the energy deposition in the vicinity of the sheath is also seen by Kawamura *et al* [23] in their self-consistent PIC simulation of RF-CCP discharges. Figure 4 also indicates the fact that stochastic heating decreases with an increasing order of sinusoidal current waveform (i.e. decreasing pulse width). This can be understood in terms of pulse shape (i.e. $\partial J/\partial t$, figure 1) which gets sharper with increasing α (equation (1)) and carries a smaller positive current (i.e. small area enclosed in the expanding/collapsing phase), responsible for smaller sheath heating. It is necessary to clarify here that the simulation results (S_{stoc}) include the heating contributions from both [34] namely the dc sheath part S_{dc} (i.e. floating sheath) and the applied RF (S_{rf}) current source. The analytical expression for the stochastic heating in a collisionless regime in the case of a CCP discharge [23] however refers to a purely applied RF source (no dc contribution) and becomes zero for $J_0 = 0$. In

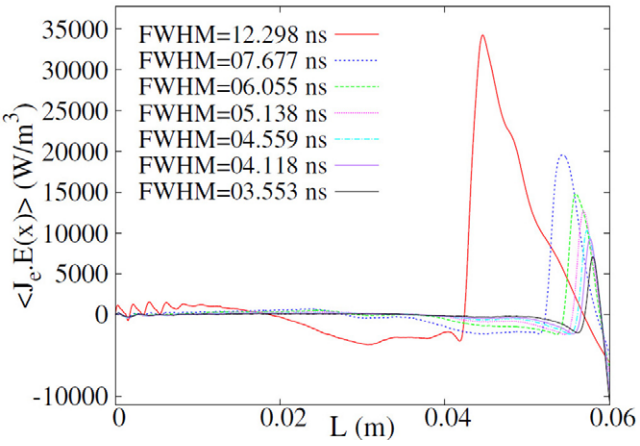

Figure 4. Space evolution of the time-averaged sheath heating ($\langle J.E \rangle$) for different pulse widths corresponding to a different order sinusoidal current driven source.

the absence of an RF source, the loss of high energy charged plasma particles to the electrode contributes to the negative heating (S_{dc}, in the proximity of the dc sheath) which effectively cools the plasma near the electrode.

The steady-state stochastic heating, averaged over space (system length) and time (over one RF period) corresponding to the applied higher order sinusoidal profile as a function of mean width (FWHM) is depicted in figure 5. In order to link our simulation results for average collisionless heating with analytical prediction (equations (14)–(16)), relevant dc heating associated with the floating sheath has been excluded from the total collisionless heating (S_{stoc}) obtained from the simulation results and only the contribution from the RF part (S_{rf}) is displayed in this figure; the magnitude of S_{dc} ($\sim -12\,\mathrm{W\,m^{-2}}$), corresponding to $J_{rf} = 0$ has been taken from the simulation. The analytical results for the average sheath heating based on the Lieberman (S_{GL}, equation (14)) and

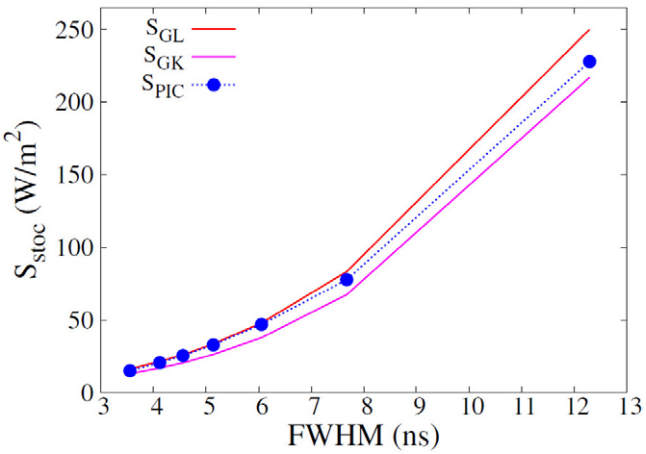

Figure 5. Average sheath heating (S_{stoc}) as a function of pulse width corresponding to different order sinusoidal current waveforms.

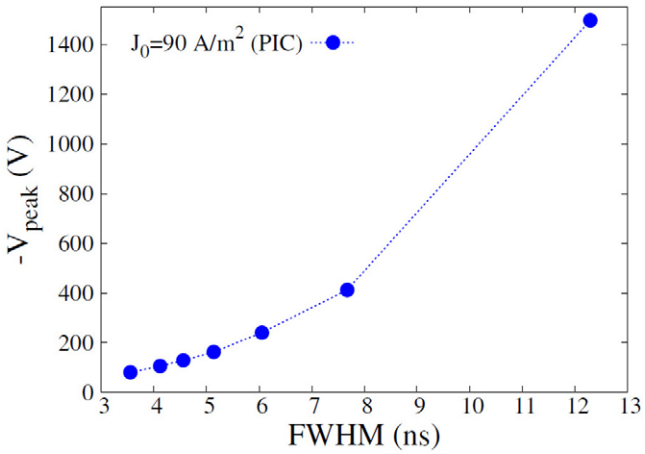

Figure 6. Maximum potential drop ($-V_{peak}$) across sheath as a function of pulse width corresponding to various order sinusoidal current profiles.

Kaganovich (S_{GK}, equation (16)) treatment has been depicted by continuous red and magenta solid lines while the simulation data is shown by blue dots. The average heating is seen to increase with increasing mean width of the pulse (FWHM); this nature is a consequence of a larger potential drop ($-V_{peak}$) across the sheath for the large pulse width, as illustrated in figure 6. The dependence of the potential drop across sheath on α (i.e. FWHM), is in conformance with the analytical prediction of mean electric potential ($\overline{\varphi}$) in figure 2(c). Larger potential drops across the sheath leads to larger kicks to the electrons in the sheath expansion phase and consequently gives larger heating. The analytical results display the fact that both S_{GL} and S_{GK} decrease and approach each other asymptotically with a decreasing pulse width; the simulation results are seen to be in very good agreement with the Lieberman prediction for higher order sinusoidal waveforms. Further, the peak potential (figure 6) increases with increasing FWHM and it takes its largest value in the case of the pure sinusoidal waveform; this is in conformance with the largest stochastic heating obtained in this case (figure 3, for $\alpha = 0$). It can be seen from the figures (i.e. figure 5) that the average heating associated with an RF source always takes positive values and leads to positive heating of the plasma. An important feature which can be extracted from the figures (figure 5 and 6), shows that the sheath heating and hence the potential drop across sheath can be tuned by varying the pulse mean width (FWHM) by a tuning parameter α. This potential drop across the sheath usually drives the ion energy depositing over the substrate in CCP discharges. Although this analysis only takes account of a periodic sinusoidal profile, this conceptual basis can be extended for any periodic pulse profile for current-driven CCP discharges.

In summary, on the basis of analytical formulation and PIC simulation it is shown that collisionless sheath heating can be controlled by varying the pulse width in current-driven CCP discharges; consequently it leads to an additional control over the potential drop across the sheath and hence the ion energy. A current-driven RF source characterized by a higher order sinusoidal profile is considered where the pulse width is tuned by parameter α. The analytical predictions are in very good agreement with the simulation results; the analysis for the pure sinusoidal pulse (i.e. $\alpha = 0$) is found to display the maximum sheath heating among all the profiles (namely $\alpha > 0$) considered herein. The technique to utilize the pulse width as a tuning parameter to control ion energy allows a level of control over the power deposition over the electrode in CCP discharges and is of relevance to the etching/deposition processes in numerous material processing applications. The outcome of the numerical analysis is strictly relevant to the systems operating in a collisionless regime, and displays a qualitative agreement with the analytical prediction of the collisionless sheath heating of electrons in current-driven CCP discharge sources.

Acknowledgments

This work is supported by Department of Science & Technology (DST), Government of India via Projects GITA/ DST/ TWN/ P-56/ 2014, DST-JC Bose Fellowship and YOS Professor PKK 92-14.

References

[1] Lieberman M A and Lichtenberg A J 2005 *Principles of Plasma Discharges and Materials Processing* (New York: Wiley)
[2] Heil B G, Czarnetzki U, Brinkmann R P and Mussenbrock T 2008 *J. Phys. D: Appl. Phys.* **41** 165202
[3] Heil B G, Schulze J, Mussenbrock T, Brinkmann R P and Czarnetzki U 2008 *IEEE Trans. Plasma Sci.* **36** 1404
[4] Schulze J, Schungel E and Czarnetzki U 2009 *J. Phys. D: Appl. Phys.* **42** 092005
[5] Donko Z, Schulze J, Heil B G and Czarnetzki U 2009 *J. Phys. D: Appl. Phys.* **42** 025205
[6] Schulze J, Schungel E, Donko Z and Czarnetzki U 2011 *Plasma Sources Sci. Technol.* **20** 015017
[7] Derzsi A, Korolov I, Schungel E, Donko Z and Schulze J 2013 *Plasma Sources Sci. Technol.* **22** 065009
[8] Donko Z, Schulze J, Hartmann P, Korolev I, Czarnetzki U and Schungel E 2010 *Appl. Phys. Lett.* **97** 081501

[9] Schulze J, Schungel E, Czarnetzki U, Gebhardt M, Brinkmann R P and Mussenbrock T 2011 *Appl. Phys. Lett.* **98** 031501
[10] Schungel E, Schulze J, Donko Z and Czarnetzki U 2011 *Phys. Plasmas* **18** 013502
Heil B G, Czarnetzki U, Brinkmann R P and Musserbrock T 2008 *J. Phys. D: Appl. Phys.* **41** 165202
[11] Johnson E V, Verbeke T, Vanel J C and Booth J P 2010 *J. Phys. D: Appl. Phys.* **43** 412001
[12] Donko Z 2011 *Plasma Sources Sci. Technol.* **20** 024001
[13] Lafleur T and Booth J P 2012 *J. Phys. D: Appl. Phys.* **45** 395203
[14] Lafleur T, Delattre P A, Johnson E and Booth J P 2012 *Appl. Phys. Lett.* **101** 124104
[15] Delattre P A, Lafleur T, Johnson E and Booth J P 2013 *J. Phys. D: Appl. Phys.* **46** 235201
[16] Coumou D J, Clark D H, Kummerer T, Hopkins M, Sullivan D and Shannon S 2014 *IEEE Trans. Plasma Sci.* **42** 1880
[17] Lieberman M A 1988 *IEEE Trans. Plasma Sci*. **16** 638
[18] Kaganovich I D, Kolobov V I and Tsendin L D 1996 *Appl. Phys. Lett.* **69** 3818
[19] Turner M M 1998 *Electron Kinetics and Application of Glow Discharges NATO ASI Series* B vol **367** (New York: Kluwer)
[20] Gozadinos G, Turner M M and Vender D 2001 *Phys. Rev. Lett.* **87** 135004
[21] Kaganovich I D, Polomarov O V and Theodosiou C E 2004 *Phys. Plasmas* **11** 2399
[22] Kaganovich I D, Polomarov O V and Theodosiou C E 2006 *IEEE Trans. Plasma Sci.* **34** 696
[23] Kawamura E, Lieberman M A and Lichtenberg A J 2006 *Phys. Plasmas* **13** 053506
[24] Turner M M 2009 *J. Phys. D: Appl. Phys.* **42** 194008
[25] Sharma S and Turner M M 2013 *J. Phys. D: Appl. Phys.* **46** 285203
[26] Sharma S and Turner M M 2013 *Plasma Sources Sci. Technol.* **22** 035014
[27] Sharma S 2013 Investigation of ion and electron kinetic phenomena in capacitively coupled radio-frequency plasma sheaths: a simulation study *PhD thesis*, Dublin City University
[28] Lafleur T, Boswell R W and Booth J P 2012 *Appl. Phys. Lett.* **100** 194101
[29] Sharma S, Mishra S K and Kaw P K 2014 *Phys. Plasmas* **21** 073511
[30] Lafleur T, Chabert P and Booth J P 2014 *Plasma Sources Sci. Technol.* **23** 035010
[31] Popov O A and Godyak V A 1985 *J. Appl. Phys.* **57** 53
[32] Godyak V A and Piejak R B 1990 *Phys. Rev. Lett.* **65** 996
[33] Gozadinos G, Vender D and Turner M M 2001 *J. Comput. Phys.* **172** 348
[34] Gozadinos G 2001 Collisionless heating and particle dynamics in radio-frequency capacitive plasma sheaths *PhD thesis*, Dublin City University
[35] Gozadinos G, Vender D, Turner M M and Lieberman M A 2001 *Plasma Sources Sci. Technol.* **10** 117
[36] Turner M M and Chabert P 2006 *Phys. Rev. Lett.* **96** 205001
[37] Turner M M and Chabert P 2006 *Appl. Phys. Lett.* **89** 231
[38] Turner M M and Chabert P 2007 *Plasma Sources Sci. Technol.* **16** 364
[39] Schulze F J 2009 Electron heating in capacitively coupled radio-frequency discharges *PhD thesis*, Ruhr University, Bochum
[40] Sharma S and Turner M M 2013 *Phys. Plasmas* **20** 073507
[41] Sharma S, Mishra S K, Kaw P K, Turner M M and Karkari S K 2015 *Contrib. Plasma Phys.* in press doi:10.1002/ctpp.201400077